

Approach and Landing Technologies for STOL Fighter Configurations

Daniel W. Banks* and John W. Paulson Jr.†
NASA Langley Research Center, Hampton, Virginia

Providing next-generation fighter aircraft with short takeoff and landing capability will require effective high-lift systems, methods of providing adequate longitudinal trim and control, and thrust reversers compatible with advanced configurations. Recent wind tunnel tests in the NASA Langley 4 × 7-m tunnel have provided the opportunity to investigate some promising technologies for providing this short takeoff and landing capability. These tests include investigations of the high-lift contribution of spanwise blowing on a trailing-edge flap system, the trim capability of a blown high-lift canard, and the deceleration of a thrust reverser for ground roll reduction. This paper reviews the results of each investigation and examines the integration of these technologies on a common advanced fighter configuration to determine their compatibility and the resulting overall performance of the configuration.

Nomenclature

a	= acceleration, ft/s ²
\mathcal{R}	= aspect ratio, b^2/S
b	= wing span, ft
\bar{c}	= wing mean aerodynamic chord, ft
C_D	= drag coefficient, drag/ qS
$C_{D,\min}$	= minimum drag coefficient
C_L	= lift coefficient, lift/ qS
$C_{L,0}$	= lift coefficient at $\alpha=0$ deg
$C_{L,\alpha}$	= lift-curve slope, $\partial C_L/\partial\alpha$
C_m	= pitching-moment coefficient, pitching moment/ $qS\bar{c}$
C_{m_α}	= longitudinal stability derivative, $\partial C_m/\partial\alpha$
$C_{m_\alpha=0 \text{ deg}}$	= pitching-moment coefficient at zero angle of attack
C_T	= thrust coefficient, thrust/ qS
C_T	= thrust coefficient, thrust/ qS
$C_{T,\text{pri}}$	= primary nozzle thrust coefficient
C_μ	= ideal thrust coefficient, ideal thrust/ qS
$C_{\mu,c}$	= canard blowing coefficient
$\Delta C_{D,\Gamma}$	= thrust-induced increment in drag coefficient, $C_D _{C_T>0} - C_T \cos\alpha - C_D _{C_T=0}$
$\Delta C_{m,\Gamma}$	= thrust-induced increment in pitching-moment coefficient, $C_m _{C_T>0} - C_m _{C_T=0}$
$\Delta C_{L,\Gamma}$	= thrust-induced increment in lift coefficient, $C_L _{C_T>0} - C_T \sin\alpha - C_L _{C_T=0}$
g	= gravitational constant, 32.174 ft/s ²
i_c	= canard incidence angle, deg
q	= freestream dynamic pressure, psf
S	= reference wing area, ft ²
T/W	= thrust-to-weight ratio
W/S	= wing loading, psf

X_g	= ground roll, ft
α	= angle of attack, deg
γ	= flight-path angle, deg
δ_f	= flap deflection angle, deg
$\delta_{f,c}$	= canard flap deflection angle, deg
δ_K	= Krueger flap deflection angle, deg
δ_N	= primary nozzle deflection angle, deg
Λ_c	= cascade nozzle angle, deg
μ	= friction coefficient
ρ	= density, slug/ft ³

Introduction

GOOD short takeoff and landing (STOL) fighter configurations must be capable of generating high levels of lift coefficient on approach to obtain the minimum possible touchdown velocity, be able to trim the associated pitching moments, and also have effective levels of reverse thrust available shortly after touchdown for minimum ground roll. Obtaining high levels of lift coefficient is normally limited by both the angle of attack that aircraft can maintain near the ground (i.e., tail-strike angle) and the ability to maintain longitudinal trim, particularly to accommodate powered lift effects that tend to produce large nose-down pitching moments due to the generation of lift behind the aircraft center of gravity.

For any given configuration, the ground roll is dependent on the velocity at touchdown and the magnitude of the retarding force that can be applied after touchdown. The velocity on approach (that ends with touchdown) is a function of the lift coefficient that a configuration can generate, and its wing loading. The retarding force to decelerate is usually produced with wheel brakes in combination with one or more of the following: drag chutes, speed brakes, arresting wires, and thrust reversers. Each have their own merits and disadvantages. Only the thrust reverser is capable of producing the same high magnitude of deceleration in any weather (rain, snow, ice) and is immediately reusable. Obtaining effective reverse thrust within a short time after touchdown requires that the mechanism for reversing the jet flow be fast acting and the needed levels of reverse thrust be available at that time. Present-technology jet engines normally require several seconds to reach full military power from low power settings due to the high inertia of the rotating machinery. Therefore, in

Presented as Paper 84-0334 at the AIAA 22nd Aerospace Sciences Meeting, Reno, Nev., Jan. 9-12, 1984; received March 15, 1984; revision received Dec. 1, 1984. This paper is declared a work of the U.S. Government and therefore is in the public domain.

*Aerospace Technologist. Member AIAA.

†Head, High-Performance Military Aircraft Group, Subsonic Aerodynamics Branch, Low-Speed Aerodynamics Division. Member AIAA.

order to have the needed levels of reverse thrust available on touchdown, the engines must be operating at near military power on approach. Powered-lift systems may be able to use the available engine power to generate lift without producing unwanted excess thrust on approach.

To analyze the compatibility and performance of an advanced configuration with trimmed high lift and an effective thrust reverser, the incremental effects of the individual technologies tested on similar configurations were consolidated into one common airframe. The design approach condition for the aircraft was an angle of attack of 12-16 deg, a glide slope of 3-6 deg, and an engine power setting equivalent to a sustained thrust coefficient of 0.6-1.0. An effective thrust reverser was deemed to be a mechanism that could convert 50% of military power to reverse thrust.

The effect of approach lift coefficient on landing ground roll (Fig. 1) shows that even relatively small increases in approach lift coefficient can provide significant reductions in ground roll. Also shown in Fig. 1 is the fact that availability of an effective thrust reverser, which can provide an additional deceleration of 0.5 g, can reduce ground roll on the order of 50%. These reductions are even more significant on wet or icy runways where wheel braking may be ineffective or negligible. The current goal for STOL fighter landing ground roll is 1000-1500 ft. To meet this goal in an all-weather environment for the next-generation fighter, it will be desirable to have a combination of these technologies (high lift, adequate pitch trim, and effective thrust reverser) integrated into these designs.

Spanwise Blowing on a Trailing-Edge Flap

The ability of underwing spanwise blowing on a trailing-edge flap system to produce induced lift was investigated in the Langley 4- \times 7-m tunnel on a Langley wing-canard research model.^{1,2} The wing-canard model (Fig. 2) was modified to closely resemble an advanced fighter configuration.³ The concept of underwing spanwise blowing on a trailing-edge flap system is quite different from the conventional method of blowing above the wing near the leading edge to induce a vortex that will reattach the flow at high angles of attack. Blowing spanwise along the underside of the wing, the jet will be turned chordwise by the freestream and turned downward by the flap thereby inducing circulation to generate lift in a manner similar to externally blown flaps.

The secondary nozzles used to generate the spanwise blowing were two-dimensional cascades located just upstream of the primary nozzles as indicated in Figs. 3 and 4. The diagram in Fig. 3 and photo in Fig. 4 show the basic design and placement of the spanwise blowing nozzles cascades and trailing-edge flap. Figure 5 shows an oil-flow pattern of the underside of the wing with spanwise blowing. The strong influence of the spanwise jet on both the flap and wing is shown. Tests were

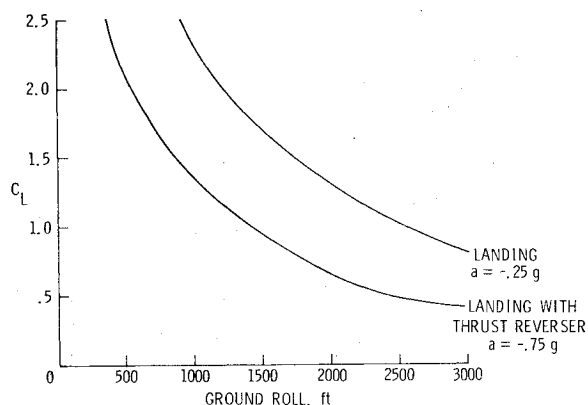


Fig. 1 Effect of approach lift coefficient and thrust reverser on landing ground roll for fighter aircraft, dry runway and antiskid braking system.

conducted to investigate various combinations of spanwise vector angle, flap deflection, and thrust coefficients. Spanwise vector angles of -30, 0, 30, 45, and 60 deg (Fig. 3) were tested at thrust coefficients from 0 to 2.1. Inboard and outboard flaps were deflected in combinations of 0, 26, and 45 deg as shown in Fig. 3. The detailed results of each configuration are published in other works^{1,4} and, therefore, will not be reported here. The configuration which seemed most appropriate for the desired approach condition was one with the spanwise nozzles vectored at an angle of 30 deg (parallel to the flap hinge line) and both inboard and outboard flaps deflected 26 deg (see Fig. 3). With the spanwise blowing vector angle of 30 deg, the axial thrust component is one-half total thrust produced. This allows the engine to operate at a high power setting on approach, which is attractive for quick thrust reverse response.

The effect of flap deflection on longitudinal aerodynamics is shown in Fig. 6 for the basic model without spanwise blowing. The main effect of flap deflection is an increase in $C_{L,0}$ of about 0.35, an increase in nose-down pitching moment $C_{m_{\alpha=0\text{ deg}}}$ of 0.21, and an increase in $C_{D,\text{min}}$ of 0.06. It also had the effect of being destabilizing in pitch, as shown by the slight increase in the positive slope of C_m vs α (the advanced configuration was designed for 15% static instability).

Figure 7 shows the thrust-induced aerodynamics for the wing-canard fighter configuration as a function of ideal thrust coefficient for two angles of attack (12 and 16 deg). In the C_μ range of interest, 0.6 to 1.0, at angles of attack of 12 and 16 deg the induced lift $\Delta C_{L,T}$ (Fig. 7) ranges from 0.16 to 0.24. At higher thrust coefficients the spanwise flow is turned less by the freestream, and, therefore, affects less of the flap and pro-

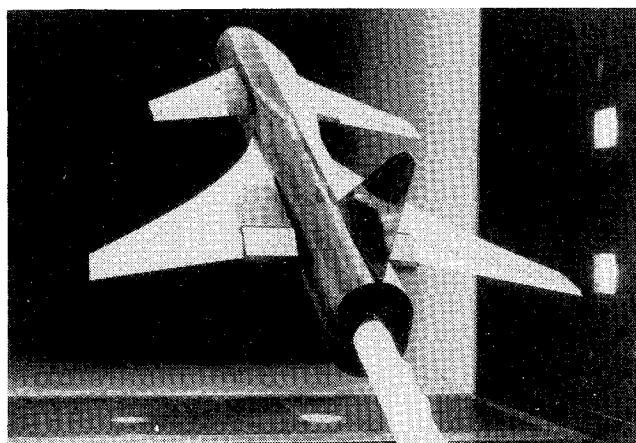


Fig. 2 Wing-canard fighter model installed in the Langley 4- \times 7-m tunnel.

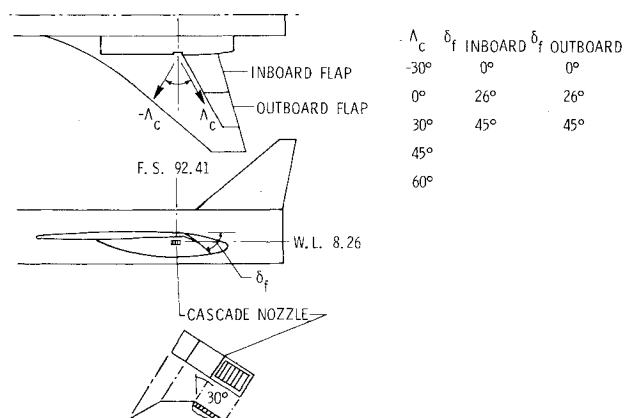


Fig. 3 Location of cascades under trailing-edge flap on the wing-canard fighter model.

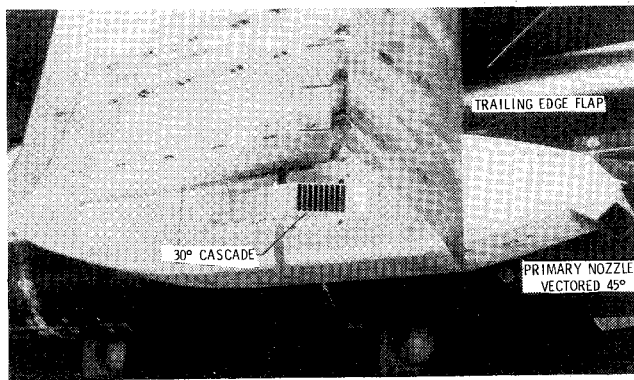


Fig. 4 Spanwise blowing cascade nozzle and trailing-edge flap system on the wing-canard fighter model.

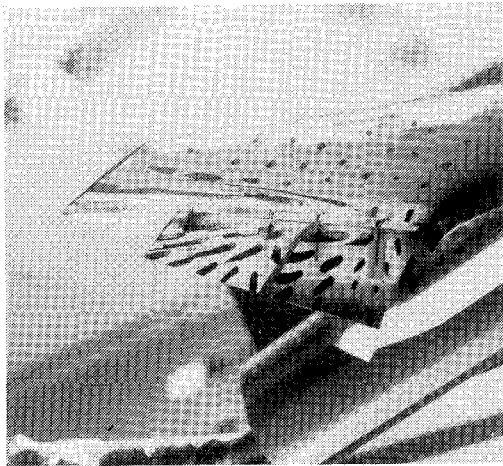


Fig. 5 Oil-flow pattern on the wing-canard fighter model with underwing spanwise blowing ($\delta_N = 45$ deg, $\delta_f = 45/26$ deg).

duces less induced lift. At very high thrust coefficients and low angle of attack the jet can miss the flap completely and have a detrimental effect on induced lift. Overall spanwise blowing generates favorable amounts of induced lift which is favorable for a STOL approach.

The thrust-induced drag $\Delta C_{D,\Gamma}$ in Fig. 7 behaves as would be expected—increasing constantly with increases in induced lift. The drag levels produced are favorable for the approach condition. The thrust-induced pitching moment $\Delta C_{m,\Gamma}$ in Fig. 7 indicates that the nose-down increment in pitching moment is not as severe as many methods of powered lift, but nonetheless is higher than most conventional control surfaces can trim.⁵

Using the spanwise blowing nozzles as thrust reversers after touchdown would have several advantages. The main nozzle could be of simple design (i.e., axisymmetric, nonvectoring, nonreversing), reducing cost, weight, and complexity. The spanwise blowing nozzles also splay the reverse thrust out laterally, thereby avoiding ground impingement and lessening the chance of foreign object damage and hot gas ingestion.

With the 30 deg spanwise blowing nozzles used on approach, the engine power setting could be maintained near military power due to the sideforce cancellation. After touchdown, the spanwise nozzles could be rotated laterally forward with very little increase in engine power necessary to achieve an effective level of reverse thrust. Further, although not tested in ground effect, the underwing blowing could create suckdown forces in this condition which would further aid in decelerating the aircraft by increasing the normal force on the wheels, thereby increasing rolling resistance and braking effectiveness.

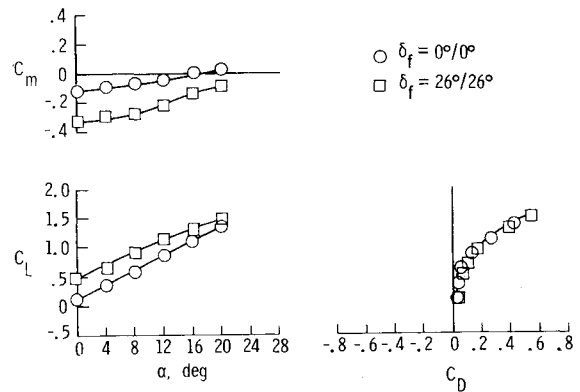


Fig. 6 Effect of flaps on the longitudinal aerodynamics of the wing-canard fighter model.

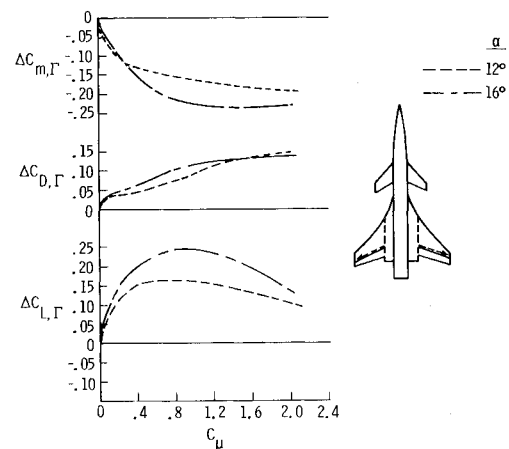


Fig. 7 Thrust-induced longitudinal aerodynamics with underwing spanwise blowing.

High-Lift Canard

As part of a joint investigation of an advanced technology fighter configuration by NASA, Grumman, and the Air Force, an advanced technologies for tactical aircraft (AT-TAC) model was tested with a blown high-lift canard.⁵ This canard was designed to produce high lift and, therefore, large nose-up pitching moments to trim the large nose-down pitching moments created by powered lift and vectored thrust. Canard high lift was generated in much the same fashion as conventional powered high-lift wings, that is, chordwise blowing to maintain flow attachment on the trailing-edge flap and a leading-edge flap to delay leading-edge separation.

The model shown in Fig. 8 in the 4- \times 7-m tunnel was tested with and without a canard leading-edge device (Krueger flap) at various canard trailing-edge flap angles with boundary-layer control blowing at the knee of the flap to maintain attached flow through large flow turning angles.

The maximum nose-up aircraft moment from the canard at the approach condition, $\alpha = 12$ -16 deg, was obtained with the Krueger leading edges, the trailing-edge flaps deflected 30 deg, canard incidence i_c of 0 deg, and moderate blowing $C_{\mu,c} = 0.021$, as indicated in Fig. 9. Larger blowing coefficients can increase the available lift of the canard, but increasing the blowing coefficient past the point needed to maintain attached flow on the canard flap will create a jet sheet that increases the downwash at the wing further, thereby decreasing wing lift. In most cases, the total lift of the configuration (wing and canard) remains constant as the canard lift is increased. That is, the downwash field of the canard tends to unload that portion of the wing directly behind it in proportion to the lift the canard is generating.² This, along with a declining benefit in

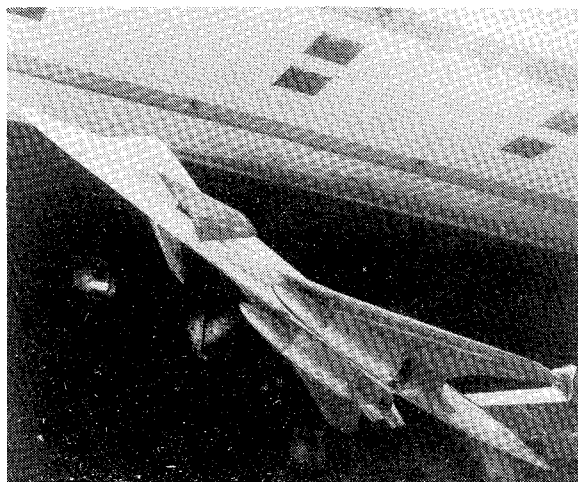


Fig. 8 ATTAC model with high-lift blown canard.

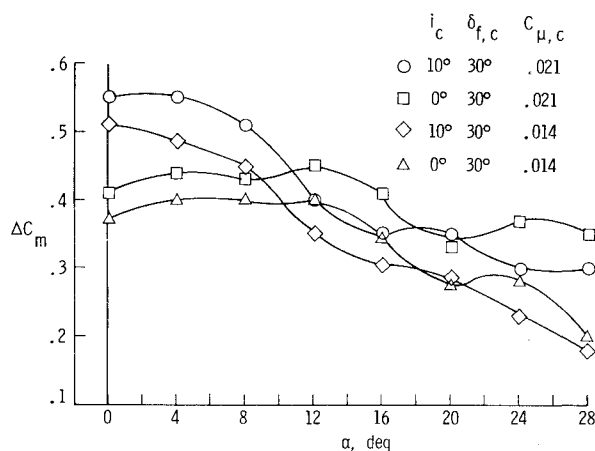


Fig. 9 Aircraft pitching-moment increment for the blown high-lift canard.

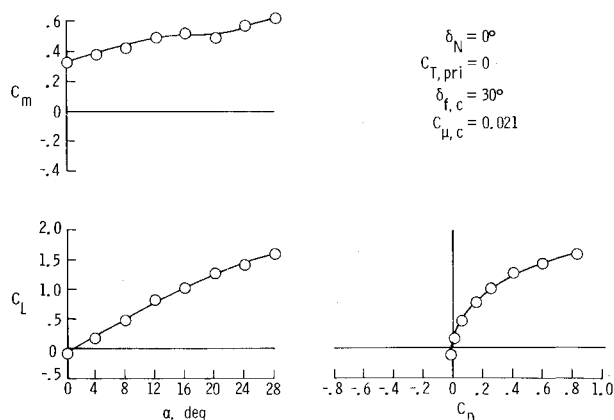


Fig. 10 Longitudinal aerodynamics of the ATTAC model with the optimum blown high-lift canard configuration.

canard lift per unit thrust, make larger blowing coefficients unattractive.

The longitudinal aerodynamics of the ATTAC configuration are shown in Fig. 10 with the optimum canard configuration for approach (Krueger leading edge, $\delta_{f,c} = 30^\circ$, $C_{\mu,c} = 0.021$, and $i_c = 0^\circ$), but with the main nozzle unpowered ($\delta_N = 0^\circ$). This was considered the baseline approach configuration to integrate with the spanwise-blowing concept and trailing-edge flap system.

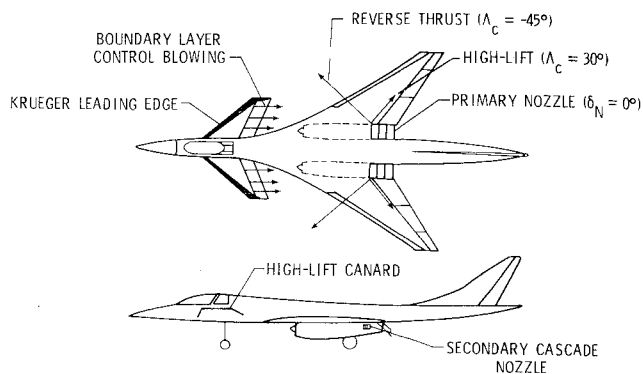


Fig. 11 Advanced fighter configuration with high-lift blown canard and underwing spanwise blowing.

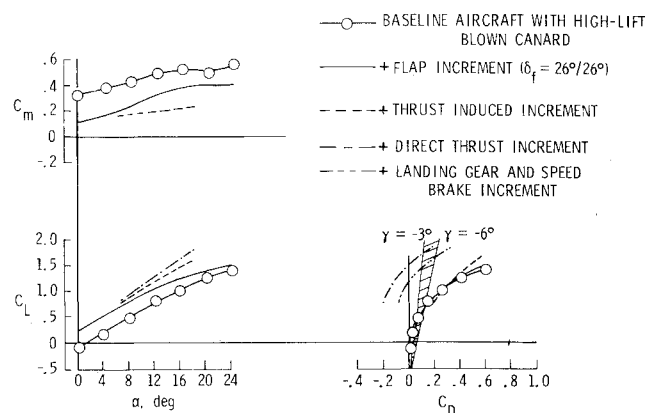
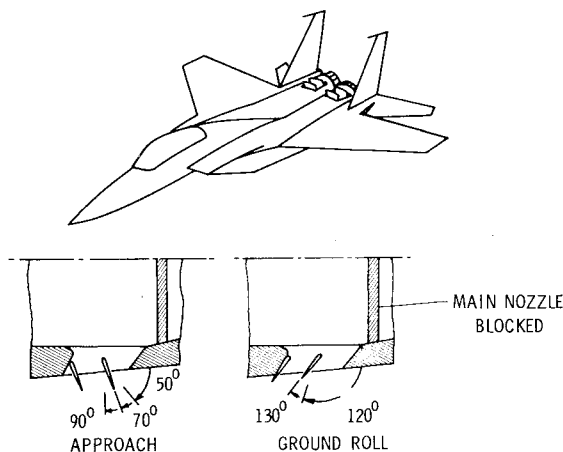
Fig. 12 Longitudinal aerodynamics of conceptual advanced fighter configuration with spanwise blowing, and high-lift blown canard at $C_T = 0.8$.

Fig. 13 Rotating vane thrust reverser on an F-15 model in approach and ground roll configurations.

Approach Configuration

The wing-canard model used to test the spanwise blowing concept had been modified to closely resemble the Grumman ATTAC model. Therefore, it is felt that the incremental data on spanwise blowing derived from the Langley wing-canard model can be applied to the ATTAC model characteristics to examine the combined aerodynamics. The combination of spanwise blowing for powered lift, rotation of the spanwise blowing cascades for thrust reverse, and a blown high-lift canard for trim are design elements very compatible for a conceptual advanced fighter configuration.

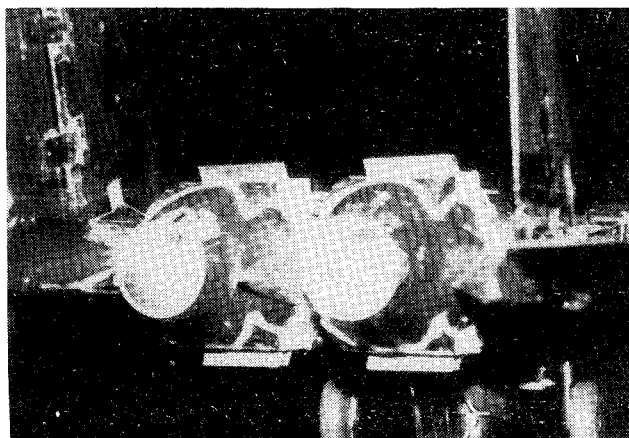


Fig. 14 Rotating vane thrust reverser in approach configuration on F-15 model.

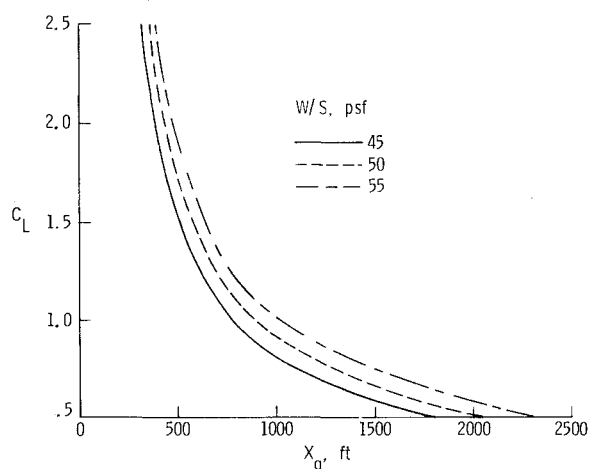


Fig. 15 Calculated landing ground roll for a conceptual advanced fighter with a 50% effective thrust reverser on a dry runway.

The conceptual advanced fighter configuration is shown in a possible approach condition with spanwise blowing in Fig. 11, and the longitudinal aerodynamic characteristics of the configuration are shown in Fig. 12. The increments due to underwing spanwise blowing on the trailing-edge flap system, derived from the Langley wing-canard model, were added to the baseline ATTAC configuration with the optimum canard configuration. The data in Fig. 12 also include the effect of landing gear and speed brake on drag.⁶ At the designated approach angle of attack of 14 deg and $C_T = 0.8$, $C_L = 1.48$, and the L/D is such that the glide slope would be 3 deg. With these conditions and a wing loading of 50 psf, such a configuration would be in an equilibrium approach condition at approximately 100 knots (i.e., $W/qS \sin \gamma = C_D$, and $W/qS \cos \gamma = C_L$ where C_L and C_D include direct thrust components). With the high-lift canard, the configuration at the approach condition has a margin of available pitching moment above trim retained for pitch control. Unloading the canard, to obtain pitch trim, will result in an equal increase of lift on the wing behind the canard due to the decreased downwash from the canard. For this reason, the lift coefficient at the trim point is much the same as that for the untrimmed condition depicted in Fig. 12.

The spanwise blowing cascade nozzles are very similar to the rotating vane thrust reverser nozzles previously tested on a 13%-scale F-15 configuration shown in Figs. 13 and 14.⁴ The rotating vane thrust reverser showed significant effectiveness. Therefore, the similar nozzle used on the spanwise-blowing concept should be a reasonable thrust reverser which would give performance similar to the rotating vane. Because the

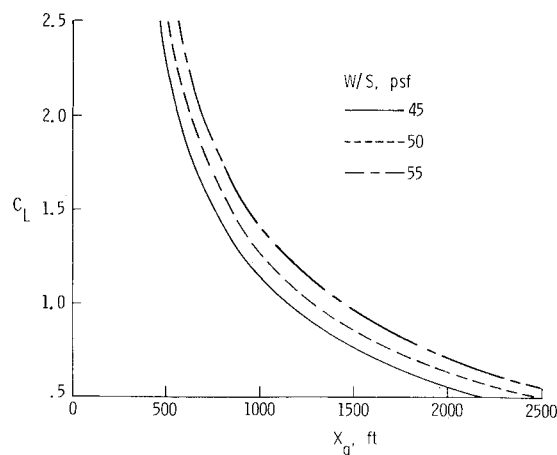


Fig. 16 Calculated landing ground roll for a conceptual advanced fighter with a 50% effective thrust reverser on a wet runway.

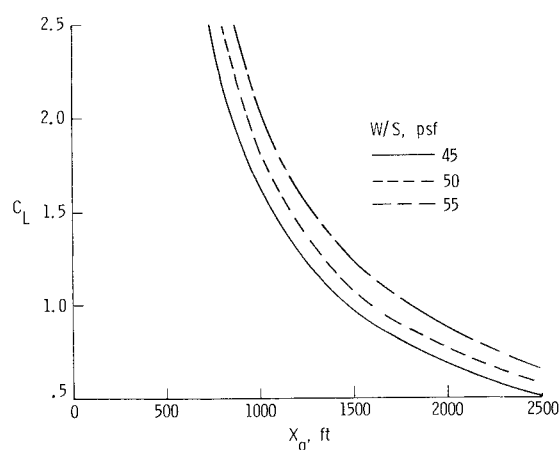


Fig. 17 Calculated landing ground roll for a conceptual advanced fighter with a 50% effective thrust reverser on an icy runway.

spanwise blowing nozzles are splayed laterally, the reingestion concerns due to the reverse jet impinging on the ground that limit the minimum velocity for thrust reverser operation may be eliminated.

Landing Ground Roll Calculation

Figure 15 shows calculated ground roll plotted as a function of approach lift coefficient for three representative wing loadings for this class of aircraft (dry runway). It is assumed the aircraft is equipped with a 50% effective thrust reverser capable of producing full reverse thrust 1 s after touchdown (in addition to wheel braking) which can be maintained down to 10 knots. The friction coefficient μ was chosen to represent that of an antiskid braking system which varied from 0.025 above 140 knots to 0.54 at 0 knot. The field length calculation procedure based on wind tunnel data has been validated with current fighter aircraft performance.⁴ Figure 16 depicts the same scenario except the runway condition is assumed to be wet and ungrooved. As shown, the landing ground roll for an approach $C_L = 1.48$, is less than 650 ft for the dry runway case, 950 ft for the case of a wet runway, and 1300 ft with no available wheel braking. In Fig. 17, the aircraft is assumed to have no wheel braking which is the worst case (ice). Touchdown dispersion and reduced aircraft performance will add to the actual runway field length required. This configuration seems to provide for landing ground rolls less than 1500 ft for approach lift coefficients on the order of 1.5 for all runway conditions.

Conclusions

A series of wind-tunnel investigations have been conducted to determine the ability of several advanced technology concepts to provide STOL approach and landing capability. The concept of using underwing spanwise-blowing on a trailing-edge flap system, and an effective thrust reverser integrated into an advanced conceptual fighter configuration with a high-lift blown canard was analyzed to determine the compatibility of the concepts and overall configuration performance. The analysis of the data indicates that the integration of various technologies could provide useful STOL capability.

The concept of underwing spanwise blowing was shown to provide moderate levels of induced lift when used in conjunction with a trailing-edge flap system. It also can provide the opportunity to spoil excess thrust which can allow higher power settings on approach. The spanwise blowing nozzles vectored forward could provide a useful means of providing reverse thrust without ground impingement and therefore decreased change of foreign object damage and hot gas ingestion.

A blown high-lift canard was found to have the capability to trim the large nose-down pitching moments associated with the spanwise-blowing concept on an advanced fighter configuration. Further, it provided adequate levels of pitching moment for control above that needed for trim.

Integrating these technologies into one conceptual configuration indicates the potential for a trimmed STOL approach condition with high power settings, and effective reverse thrust to provide landing ground rolls on the order of 1000 ft.

References

- ¹Paulson, J. W. Jr., Quinto, P. F., and Banks, D. W., "An Investigation of Trailing Edge Flap Spanwise Blowing Concepts on an Advanced Fighter Configuration," NASA TP-2250, Feb. 1984.
- ²Paulson, J. W. Jr. and Thomas, J. L., "Summary of Low-Speed Longitudinal Aerodynamics of Two Powered Close-Coupled Wing-Canard Fighter Configurations," NASA TP-1535, Dec. 1979.
- ³Bavitz, P. C. M. Sturm, T. Ervolina, D. Reichel, V. Cimina, N. Kirschbaum, E. Toscano, and F. Shephard, "Configuration Development of Advanced Fighters, Volumes 1-4, Executive Summary," AFWAL-TR-80-3142, Vol. 1, Nov. 1980.
- ⁴Paulson, J. W. Jr., Banks, D. W., and Quinto, P. F., "Effects of Spanwise Blowing and Reverse Thrust on Fighter Low-Speed Aerodynamics," *Journal of Aircraft*, Vol. 20, Feb. 1983, pp. 159-164.
- ⁵Paulson, J. W. Jr., Gatlin, G. M., Quinto, P. F., and Banks, D. W., "Trimming Advanced Fighter for STOL Approachers," *Journal of Aircraft*, Vol. 20, Nov. 1983, pp. 957-962.
- ⁶Hoerner, S. F., "Fluid-Dynamic Drag," Hoerner Fluid Dynamics, Brick Town, N. J., 1965.

From the AIAA Progress in Astronautics and Aeronautics Series . . .

TRANSONIC AERODYNAMICS—v. 81

Edited by David Nixon, Nielsen Engineering & Research, Inc.

Forty years ago in the early 1940s the advent of high-performance military aircraft that could reach transonic speeds in a dive led to a concentration of research effort, experimental and theoretical, in transonic flow. For a variety of reasons, fundamental progress was slow until the availability of large computers in the late 1960s initiated the present resurgence of interest in the topic. Since that time, prediction methods have developed rapidly and, together with the impetus given by the fuel shortage and the high cost of fuel to the evolution of energy-efficient aircraft, have led to major advances in the understanding of the physical nature of transonic flow. In spite of this growth in knowledge, no book has appeared that treats the advances of the past decade, even in the limited field of steady-state flows. A major feature of the present book is the balance in presentation between theory and numerical analyses on the one hand and the case studies of application to practical aerodynamic design problems in the aviation industry on the other.

Published in 1982, 669 pp., 6×9, illus., \$45.00 Mem., \$75.00 List

TO ORDER WRITE: Publications Dept., AIAA, 1633 Broadway, New York, N.Y. 10019